Extremum-seeking Control with Adaptive Excitation:

Application to a Photovoltaic System

Anouer Kebir, *Student Member, IEEE*, Lyne Woodward, *Member, IEEE*
and Ouassima Akhrif, *Member, IEEE*

Abstract — **The objective of this study is to improve the performance of the extremum-seeking control (ESC) technique in terms of time and accuracy of convergence towards the optimum operating point of a dynamic system subject to the effect of external disturbances. More precisely, the idea is to reduce the undesirable effect of time scale separation in ESC on the performance of the closed loop system. The method consists in adaptively controlling the excitation signal amplitude using a neural network (NN) model, which gives a real-time estimate of the optimal operating point based on the measurement of the external disturbances. Stability of the proposed ESC with adaptive excitation, referred to in the following as $\mathbf{ESC_a}$, is demonstrated. The superiority of $\mathbf{ESC_a}$ compared to ESC in terms of accuracy and time of convergence to the optimum is demonstrated both theoretically and experimentally, in the case of the optimization of a photovoltaic panel system (PV).**

***Index Terms*— Extremum-Seeking Control, Neural Networks, Optimization, Photovoltaic System.**

I. INTRODUCTION

THE increasing complexity of engineering systems has led to numerous optimization challenges. Indeed, analytical solutions to nonlinear optimization problems are difficult or even impossible to obtain. ESC is a real-time optimization approach among others that addresses situations where the model and/or the cost function of the system to be optimized in its static mode are not available to the designer. In this case, the optimization methods are converted into a control problem of the estimated gradient to zero. This gradient is estimated by exciting the system from its input with an excitation signal and correlating this entry with its effect on the output of the system.

Manuscript received April 7, 2017; revised May 23, 2017; accepted August 03, 2017. This work was supported by the discovery grant program from the National Sciences and Engineering Research Council of Canada (NSERC-402620-2012).

The authors are with the Electrical Engineering Department, École de Technologie Supérieure, University of Quebec, Montreal, QC H3C 1K3, Canada (email: anouer.kebir.1@ens.etsmtl.ca, ouassima.akhrif@etsmtl.ca, lyne.woodward@etsmtl.ca).

It requires however the availability of the signals measurements of the input and the output of the system to control. A good review of literature on the ESC can be found in [1-3].

For most applications, the dynamics of the system to be optimized are nonlinear. In this case, the main difficulty of the ESC technique [4] is the requirement of multiple time scales between the dynamics of the system, the frequency of excitation and the speed of adaptation. The excitation must be an order of magnitude slower than the system dynamics to separate the effect of excitation from the dynamics of the system. Moreover, the adaptation must be slower than the excitation in order to distinguish the effect of excitation from the adaptation one. Unfortunately, these multiple separations of time scales have the effect of slowing down the convergence. In cases where the optimal operating point is moving slowly, ESC will perform correctly but if the system is submitted to frequent external disturbances, the performance achieved will be sub-optimal. In [1], the issue of the ESC technique convergence time was addressed and the requirement of time scale separation was eliminated. A dynamic compensation scheme was proposed providing a guarantee of stability, a rapid monitoring of changes of the operating point, and a measurement noise rejection. The result was limited however to optimization problems for systems with linear dynamics. Several other approaches were proposed to reduce the effect of time scale separation on the speed of convergence, but these approaches are based on specific conditions such as a priori knowledge of the objective function structure [5, 6], a linear time-invariant process [7], a system belonging to a class of well-defined non-linear systems [8] or an unknown linear system [9]. However, when real applications are considered, ESC must be applied to nonlinear systems with unknown dynamics.

External disturbances in many systems are measurable. Assuming that these disturbance measurements are available to the expert, they can be used to improve the performance of ESC [4]. Indeed, the modeling of the relation between the optimal operating point of the system and the external disturbances allows a real-time estimation of the location of the system optimum for each new measurement of the external disturbances. Based on the estimates provided by this model, it is then possible to adjust the ESC parameters in real time in order to converge more quickly and more precisely towards

the desired optimum. The parameters that have a significant effect on the convergence speed and accuracy of ESC include the initial conditions of the manipulated variable and the amplitude of the excitation signal. The sinusoidal signal is generally chosen as an excitation signal in the ESC. In [10] a proof that the choice of the shape of the excitation signal has a direct effect on the convergence rate of ESC is demonstrated. The study shows that ESC with a rectangular excitation signal is twice as fast as a sinusoidal signal and four times faster than a triangular signal. In [11] and [4], the authors indirectly controlled the initial condition at the ESC integrator, using anticipative action to improve the speed of convergence. In this paper, we perform an adaptive control of the amplitude of the excitation signal. Note that in [12], the excitation signal amplitude was also adapted but only to improve the accuracy of ESC in order to converge to a global maximum instead of a local one. Our objective on the other hand is to improve both accuracy and speed of convergence. In this paper, it is assumed that the objective function to be optimized is unimodal. Thus, the proposed approach consists in using the optimum estimation to control in real time the amplitude of the excitation signal in order to precisely and quickly follow the desired optimum operating point. The proposed model linking the external disturbance to the optimal operating point is based on a multilayer neural network structure. The stability of the proposed approach is demonstrated. A comparative study of ESC schemes with and without adaptive excitation in terms of accuracy and time convergence to the optimal operating point is also provided theoretically and experimentally in the case of power optimization of a photovoltaic panel that is subject to a measurable external disturbance represented in this case by radiation of sunlight.

The paper is organized as follows. After an introduction, Section II defines the optimization problem considered whereas Section III presents the classical ESC scheme. In Section IV the proposed ESC_a approach is presented and its stability is studied in Section V. A theoretical comparative analysis between ESC and ESC_a is performed in Section VI whereas an experimental evaluation of both methods is provided in Section VII. Finally, conclusions of the paper are presented in Section VIII.

II. Optimization problem formulation

Let us consider a dynamic system described by the following equation:

$$\dot{x} = f(x, u, d_m) \tag{1}$$

where $d_m \in \mathbb{R}^h$ is the measurable disturbances vector, $x \in \mathbb{R}^n$ is the state vector, $f: \mathbb{R}^n \times \mathbb{R} \times \mathbb{R}^h \to \mathbb{R}^n$ is unknown and $u \in \mathbb{R}$ is the input such that:

$$u = \alpha(x, \beta) \tag{2}$$

with α being a smooth control law parameterized by the scalar β in closed loop.

The optimization problem consists in maximizing an objective function J which describes the performance of the system in static mode. Thus the optimization problem is described mathematically as follows:

$$\begin{aligned} &Max_\beta\, J(\beta) \\ &s.t. \quad \dot{x} = f(x, \beta, d_m) = 0 \end{aligned} \tag{3}$$

where $J: \mathbb{R} \to \mathbb{R}$ is unknown but can be evaluated from available measurements.

III. Extremum seeking control

ESC is a real-time optimization method that solves the problem defined in (3) while assuming that the system dynamics f and the objective function J are unknown. The method consists in exciting the system by periodic signals and observing the output behavior of the system in static mode in order to estimate and control the gradient of the objective function to zero. The ESC structure (see Fig. 1) is defined as follows:

$$\beta = \hat{\beta} + a\, sin(\omega t) \tag{4}$$

$$\dot{\hat{\beta}} = k_{ESC}\hat{g} \tag{5}$$

$$\dot{\hat{g}} = -\omega_l \hat{g} + \omega_l (J - \eta) a\, sin(\omega t) \tag{6}$$

$$\dot{\eta} = -\omega_h \eta + \omega_h J \tag{7}$$

where $a \in [a_{min}\ a_{max}]$ represents the amplitude of the excitation signal which is, in most cases, represented by a sinusoidal signal, ω is the frequency of the excitation nal, a_{min} and a_{max} are small positive constants with $a_{max} = \varepsilon a_{min}$, $\varepsilon \in \mathbb{R}$ and $\varepsilon > 1$, ω_h is the cutoff frequency of the high-pass filter used to eliminate the constant part η of J, ω_l is the cutoff frequency of the low-pass filter used to obtain the average value of the correlation between J and the excitation signal and k_{ESC} is the integral controller gain used to push the estimated gradient $\hat{g}$ to zero.

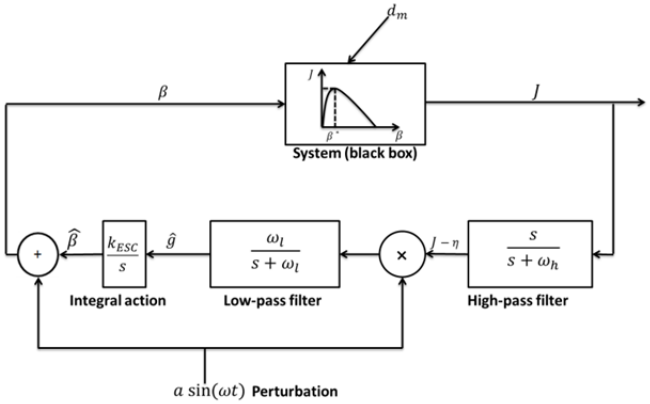

Fig. 1. Block diagram of ESC scheme.

A judicious choice of ESC parameters is essential to ensure stability and compromise between accuracy and speed of convergence to the optimal operating point. Indeed, if the system is subject to large and rapid external disturbances, these performance criteria will be degraded in the case of optimization of non-linear systems with unknown dynamics as previously shown in a microbial fuel cell application [4]. Also in [13], for the same system, the effect of the choice of k_{ESC} and a on ESC performance in terms of accuracy and speed of convergence is shown. Therefore, adapting the ESC parameters, as proposed in this paper, is essential to ensure stability and converge quickly and accurately to the optimal operating point in the presence of external disturbances.

IV. PROPOSED APPROACH: ESC_A

A. ESC_a structure

The amplitude of the ESC excitation signal is among the control parameters which have the most important effect on the precision and convergence time of the optimization method (when the amplitude decreases, the time of convergence towards the optimum increases and the precision increases around the optimum and vice versa). Thus, as in the proposed ESC_a scheme depicted in Fig. 2, if an estimate of the optimal operating point position is provided to the ESC loop, the excitation signal amplitude may be adaptively controlled, so that the amplitude becomes smaller when the operating point is near the optimum and larger when it is far from it. As a result, the ESC_a loop converges both precisely and rapidly to the desired optimal operating point.

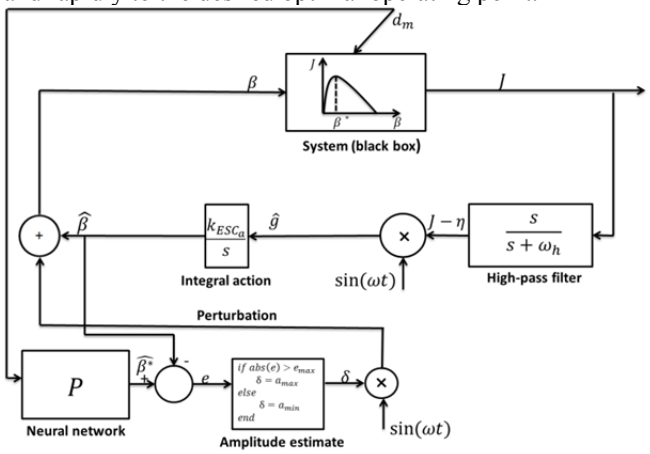

Fig. 2 . Block diagram of the proposed ESC_a.

Suppose that there exists a function $p: \mathbb{R}^h \rightarrow \mathbb{R}$ providing an estimate $\widehat{\beta^*}$ of the real optimum β^* using the measurement of the external perturbations vector d_m:

$$\widehat{\beta^*} = p(d_m). \tag{8}$$

Taking into account the estimate $\widehat{\beta^*}$, one can control the amplitude of the excitation signal according to the error e between $\widehat{\beta^*}$ and $\hat{\beta}$. Hence, the constant amplitude a in the classic ESC will be replaced by variable amplitude δ, whose expression is described by the following equations:

$$\begin{cases} \delta = a_{max} \text{ if } |e| > e_{max} \\ \delta = a_{min} \text{ if } |e| < e_{max} \end{cases} \tag{9}$$

with $e = \widehat{\beta^*} - \hat{\beta}$, $e_{max} \in \mathbb{R}$ being the maximum estimation error or switching error value prescribed by the expert with $e_{max} \rightarrow 0$ if $\widehat{\beta^*} \rightarrow \beta^*$.

Thus, equations (4), (5) and (6) of the ESC technique scheme are respectively replaced by the following equations:

$$\beta = \hat{\beta} + \delta \sin(\omega t) \tag{10}$$

$$\dot{\hat{\beta}} = k_{ESC_a} \hat{g} \tag{11}$$

$$\dot{\hat{g}} = -\omega_l \hat{g} + \omega_l (J - \eta) \delta \sin(\omega t), \tag{12}$$

with k_{ESC_a} is the ESC_a gain.

B. Modeling the function p using a Neural Network model

Most of the time, as long as real systems are considered, the relation between the optimal operating point β^* and the external perturbation d_m is highly non-linear and very difficult to identify with the laws of physics. In this situation, the Neural Networks modeling method is chosen since it requires only a limited number of input / output data in order to give a good model of the relation between d_m and β^*. Neural Networks approach is very efficient and powerful in the modeling of complex systems [14-16] whereas the use of an empirical model having a fixed structure suffers from a lack of flexibility especially in the case where there are several measurable disturbances. Thus, the identification of the model parameters becomes difficult and the optimum estimate becomes imprecise. In [4],a comparative study has been carried out between two anticipative ESC schemes using respectively a neural network model and a static linear model in the anticipation loop. The performance of the two approaches was compared through the optimization of the power delivered by a microbial fuel cell for which the measurement of the inlet substrate concentration was considered as the external perturbation. The study showed that the neural network model provides a more accurate estimate than the linear model and brought the system to its optimum with an advance of 20 days on the linear model. In addition, due to its capacity of generalization, the neural network model is able to provide an accurate approximation of the system behavior [17], starting with only a limited set of experimental data.

In the literature, there are several types of neural networks. The choice of a neural network generally rests on three characteristics: the architecture (multi-layered or not), the learning mode (supervised or unsupervised) and the learning algorithm (quasi-Newton, backpropagation, BFGS, etc.).

Since the input d_m and output β^* measurements are assumed to be available to the expert, the learning mode of the neural network will be supervised and a multi-layered perceptron with a hyperbolic tangent activation function and one hidden layer will be used to identify the function p. Moreover, the backpropagation algorithm [18] will be used during the learning phase.

Once the learning phase is completed, the model which represents the function p is described by the following equation:

$$p(d_m) = \widehat{\beta^*} = (1 - e^{-m_{NN} * W_2^T * \phi_2}) / (1 + e^{-m_{NN} * W_2^T * \phi_2}), \tag{13}$$

where:

$$\phi_2 = \begin{bmatrix} bias \\ \chi \end{bmatrix}, \tag{14}$$

χ is the vector of length c with the i^{th} element defined by the activation function of each neuron of the hidden layer, i.e.,

$$\chi(i) = (1 - e^{-m_{NN} \psi(i)}) / (1 + e^{-m_{NN} \psi(i)}), \tag{15}$$

$$\psi = W_1^T \phi_1 \tag{16}$$

$$\phi_1 = \begin{bmatrix} bias \\ d_m \end{bmatrix}, \tag{17}$$

and $W_1 \in \mathbb{R}^{bxc}$, $W_2 \in \mathbb{R}^{\lambda xq}$ are respectively the sets of synaptic weights between the neuron input and the hidden layer and between the hidden layer and the output neuron fixed after learning respectively, whereas $m_{NN} \in \mathbb{R}$ is the slope of the hyperbolic tangent activation functions ϕ_1 and ϕ_2 , b =

$h+1$ since the number of input neurons is equal to the number of measurable disturbances, q is the number of output neurons that is equal to 1 since the NN model estimates a single parameter (β^*), $\lambda = c+1$ with c being the number of neurons in the hidden layer chosen by the expert, *bias* is a constant value chosen by the expert.

V. STABILITY STUDY OF ESC_A

In order to lighten the following mathematical analysis of the ESC_a stability, two small modifications are performed to the scheme shown in Fig. 2. Firstly, the amplitude of the sinusoidal signal multiplying the output of the high-pass filter is equal to 1. Secondly, the low-pass filter is removed.

Thus,

$$\begin{cases} \dot{\hat{\beta}} = k_{ESC_a}\sin(\omega t)\left(J\left(\hat{\beta} + \delta\sin(\omega t)\right) - \eta\right) \\ \dot{\eta} = \omega_h\left(J\left(\hat{\beta} + \delta\sin(\omega t)\right) - \eta\right). \end{cases} \tag{18}$$

Assuming J admits a local maximum β^*, and β is close to it, using a Taylor series approximation we obtain:

$$J(\beta) \simeq J^* + \frac{J^{"*}}{2}(\beta - \beta^*)^2 \tag{19}$$

with $J^* = J(\beta^*)$ and $J^{"*} = \left.\frac{\partial^2 J}{\partial \beta^2}\right|_{\beta^*}$.

Thus for $\beta = \hat{\beta} + \delta\, sin(\omega t)$ around β^*:

$$\begin{cases} \dot{\hat{\beta}} = k_{ESC_a}\sin(\omega t)\left(J^* + \frac{J^{"*}}{2}(\hat{\beta} + \delta\sin(\omega t) - \beta^*)^2 - \eta\right) \\ \dot{\eta} = \omega_h(J^* + \frac{J^{"*}}{2}(\hat{\beta} + \delta\sin(\omega t) - \beta^*)^2 - \eta). \end{cases} \tag{20}$$

From the form of system (20) the averaging method is applicable (see, for example, Equations. (8.17)-(8.19) in [19]). Thus the average system of (20) is described as follows:

$$\begin{cases} \dot{\hat{\beta}}_{av} = -\delta k_{ESC_a}\frac{J^{"*}}{2}(\beta^* - \hat{\beta}_{av}) \\ \dot{\eta}_{av} = \omega_h(J^* + \frac{J^{"*}}{2}((\beta^* - \hat{\beta}_{av})^2 + \frac{\delta^2}{2}) - \eta_{av}) \end{cases} \tag{21}$$

provided that:

$$\delta k_{ESC_a} J^{"*} \ll \omega \text{ and } \omega_h \ll \omega\ . \tag{22}$$

The equilibrium point of the average system (21) is:

$$\eta_{av} = J^* + J^{"*}\delta^2/4 \tag{23}$$

$$\hat{\beta}_{av} = \beta^* \tag{24}$$

and the Jacobian matrix A evaluated at this equilibrium point $(\hat{\beta}_{av}, \eta_{av})$ is defined as follows:

$$A = \begin{bmatrix} \delta k_{ESC_a} J^{"*}/2 & 0 \\ 0 & -\omega_h \end{bmatrix} \tag{25}$$

with $\delta \in [a_{min}\ a_{max}], a_{min}, a_{max} > 0, k_{ESC_a} > 0, \omega_h > 0$, and $J^{"*} < 0$ by definition. Since the eigenvalues of the Jacobian matrix are:

$$\lambda_1 = \delta k_{ESC_a} J^{"*}/2 < 0, \tag{26}$$

$$\lambda_2 = -\omega_h < 0, \tag{27}$$

The Jacobian matrix at the equilibrium point $(\hat{\beta}_{av}, \eta_{av})$ is Hurwitz. Thus, the average system converges to $\beta^*$and is asymptotically stable. As $\beta = \hat{\beta} + \delta\sin(\omega t)$, then the perturbed system converges on average to β^*.

From (9) and (25), the average system can be presented in the form of a switching system [20] as,

$$\dot{x}(t) = A_{\sigma(t)}x(t) \tag{28}$$

where $\sigma(t): R^* \to \tau = \{1,2\}$ represents the switching law and $A_{\sigma(t)} \in \{A_1, A_2\}$ with

$$A_1 = \begin{bmatrix} a_{max}k_{ESC_a}J^{"*}/2 & 0 \\ 0 & -\omega_h \end{bmatrix} \tag{29}$$

and, $A_2 = \begin{bmatrix} a_{min}k_{ESC_a}J^{"*}/2 & 0 \\ 0 & -\omega_h \end{bmatrix}$. (30)

The switching law is described by the following system of equations:

$$\sigma(t) = \begin{cases} 1\ if\ e = \left|\hat{\beta}_{av} - \widehat{\beta^*}\right| > e_{max} \\ 2\ if\ e = \left|\hat{\beta}_{av} - \widehat{\beta^*}\right| < e_{max}\ . \end{cases} \tag{31}$$

According to (29) and (30) the two sub systems $\dot{x} = A_1 x$ and $\dot{x} = A_2 x$ are asymptotically stable, but according to [20], it is not sufficient to guarantee the stability of the system (28) during the switching from $A_1$to A_2 or from A_2 to A_1. Hence, we must study the stability of the switching system (28).

From [20], if the two sub systems are linear and asymptotically stable, we only need to demonstrate the existence of a common Lyapunov function for the two to ensure the stability of the system (28).

According to [21], a sufficient condition for the existence of a common Lyapunov function for the linear sub systems $\dot{x} = A_1 x$ and $\dot{x} = A_2 x$ is to have A_1 and A_2 being triangulable simultaneously using a non-singular transformation T.

Theorem [21]: If $A_i, (i = 1,2,\ldots\ldots M)$ are real matrices that commute pairwise (i.e $A_i A_j = A_j A_i$ for all i, j) then a matrix T exists such that TA_iT^{-1} are in triangular form. If A_i are stable matrices, a common Lyapunov function $v(x) = x^T Px$ exists for the system $\dot{x} = A_i x$.

Then, according to (29) and (30):

$$A_1 A_2 = A_2 A_1. \tag{32}$$

Thus, A_1 and A_2 are stable, commute pairwise, and the T matrix exists. Consequently a common Lyapunov function exists and the system (28) is therefore asymptotically stable.

TABLE I
CHOICE OF THE EXCITATION AMPLITUDE A IN ESC SCHEME FOR 3 DIFFERENT SITUATIONS

Situation 1		Situation 2	Situation 3
a	a_{min}	$\frac{(a_{min}+a_{\max})}{\mu}$, $\mu \in R$, $\frac{1+\varepsilon}{\varepsilon} < \mu < 1+\varepsilon$	$a_{\max}$

VI. PERFORMANCE ANALYSIS OF ESC AND ESC_A SCHEMES

A. Convergence analysis of the ESC scheme

Considering the average model of the closed loop system (Fig. 1) [13], the estimated gradient of the performance index $\hat{g}$ can be approximated as follows:

$$\hat{g} \simeq \frac{a^2}{2}J'(\hat{\beta}), \tag{33}$$

with $J'(\hat{\beta}) \equiv \frac{\partial J}{\partial \hat{\beta}}$.

Consequently, the time derivative of the input $\dot{\hat{\beta}}$ is described by:

$$\dot{\hat{\beta}} \backsimeq (k_{ESC}a^2/2)J'(\hat{\beta}). \quad (34)$$

Performing a first-order Taylor series expansion of the derivative $J'(\hat{\beta})$ around the optimum β^*:

$$\dot{\hat{\beta}} \backsimeq a^2 k_{ESC} m(\hat{\beta} - \beta^*), \quad (35)$$

with $m \equiv \frac{1}{2}\frac{\partial^2 J}{\partial \beta^2}\Big|_{\beta^*} < 0$,

one can provide a linear expression to characterize the evolution of $\hat{\beta}$:

$$\hat{\beta}(t) \backsimeq (\beta_0 - \beta^*)e^{a^2 k_{ESC} m t} + \beta^*. \quad (36)$$

Let us define T_{ESC} as the time needed, starting from an initial input β_0 for the ESC loop to approach the optimum β^* within a precision of $\pm 5\%$. Thus,

$$\hat{\beta}(T_{ESC}) \backsimeq (\beta_0 - \beta^*)e^{a^2 m k_{ESC} T_{ESC}} + \beta^* = \beta^* \pm 0.05\beta^*, \quad (37)$$

$$T_{ESC} \backsimeq \Gamma/(a\alpha_{max}) \quad (38)$$

with $\Gamma = \frac{ln(|\pm 0.05\beta^*|/|(\beta_0 - \beta^*)|)}{m}$ and, $\alpha_{max} = k_{ESC} \times a$ being the maximum combination between k_{ESC} and a chosen by the expert in order to achieve the best performance in terms of precision and time of convergence to the optimum, while respecting the stability conditions :

$$a k_{ESC} \frac{\partial^2 J}{\partial \beta^2}\Big|_{\beta^*} \ll \omega \text{ and } \omega_h \ll \omega. \quad (39)$$

Moreover, from (38) and (4) if $t \geq T_{ESC}$, the ESC control input β oscillates around the optimum β^* with a maximum error E_{ESC} that can be described as follows:

$$E_{ESC} \simeq a + 0.05|\beta^*|. \quad (40)$$

According to (33), (38) and (40), the convergence time depends on k_{ESC} and a whereas the estimated gradient and the maximum error depend only on a. Consequently, it is clear that the amplitude a which is to be chosen by the expert has a large influence on the speed of convergence and the precision. This choice can be summarized in three situations:

- *Situation* 1: the expert wants to reach the maximum of precision around the optimum.

- *Situation* 2: the expert wants to make a compromise between the minimum time of convergence and maximum precision around the optimum.

- *Situation* 3: the expert wants to reach the optimum as quick as possible.

For each of these 3 situations, the choice of the perturbation signal amplitude is done according to Table I. Note that for situation 2, the tuning parameter μ provides some flexibility to the user in the compromise to be done between precision and speed of convergence. In all cases, k_{ESC} is adjusted according to the choice of a such that $k_{ESC} = \alpha_{max}/a$.

B. Convergence analysis of the proposed ESC_a .

Let us define $T_{\mathrm{ESC_a}}$ as the time needed for the $\mathrm{ESC_a}$ scheme to converge from β_0 towards the optimum operating point β^* within a precision of $\pm 5\%$:

$$T_{ESC_a} \backsimeq ln(|\pm 0.05\beta^*|/|\beta_0 - \beta^*|)/(\delta^2 k_{ESC_a} m). \quad (41)$$

Considering $\beta_e = \widehat{\beta^*} \pm e_{max}$ as the value of the system input when the switch from $\delta = a_{max}$ to $\delta = a_{min}$ occurs, and $T_{ESC_{NN}}$ the time needed to converge from β_0 to β_e , then,

$$\hat{\beta}(T_{ESC_{NN}}) \backsimeq (\beta_0 - \beta^*)e^{a_{max}^2 k_{ESC_a} m T_{ESC\,NN}} + \beta^* = \beta_e \quad (42)$$

$$\text{and, } T_{ESC_{NN}} \backsimeq ln(|\beta_e - \beta^*|/|\beta_0 - \beta^*|)/(a_{max}^2 k_{ESC_a} m). \quad (43)$$

For t > $T_{ESC_{NN}}$ the input β oscillates around the optimum β^* with a maximum error E_{ESC_a} :

$$E_{\mathrm{ESC_a}} \simeq a_{min} + 0.05|\beta^*|. \quad (44)$$

Assuming that the Neural Network model p gives a sufficiently accurate estimate of the optimum such that the expert can choose $e_{max} \in [0 \;\; 0.05\beta^*]$, and :

$$\beta^* - 0.05\beta^* \leq \beta_e \leq \beta^* + 0.05\beta^*, \quad (45)$$

the time of convergence of $\mathrm{ESC_a}$ can be quantified as follows:

$$T_{ESC_a} \backsimeq \Gamma/(a_{max}\alpha_{max}). \quad (46)$$

A performance comparison of ESC and $\mathrm{ESC_a}$ for the three situations described in Section VI-A is provided in Table II. It can be seen that in the aforementioned situations, $\mathrm{ESC_a}$ converges either more quickly, more precisely or both to the optimum than ESC.

Note that the variation of the excitation signal from a_{min} to a_{max} could be performed as a continuous variation if desired. Doing this, however, the convergence time of the $\mathrm{ESC_a}$ scheme to the optimum is expected to be longer than the one obtained when an instantaneous variation of the excitation signal amplitude is used as it is the case in the present paper. Moreover, the stability study will be different from that proposed in section V. The system would become time variant and the stability could not be based on a switching system as it is the case right now. Instead, a Lyapunov-based approach should be followed to demonstrate stability ([22]).

TABLE II
PERFORMANCE COMPARISON OF ESC AND $\mathrm{ESC_A}$ IN THE THREE SITUATIONS

	Situation 1	Situation 2	Situation 3
Performance	$\begin{cases} T_{ESC} \gg T_{ESC_a} \\ E_{ESC} = E_{ESC_a} \end{cases}$	$\begin{cases} T_{ESC} > T_{ESC_a} \\ E_{ESC} > E_{ESC_a} \end{cases}$	$\begin{cases} T_{ESC} = T_{ESC_a} \\ E_{ESC} \gg E_{ESC_a} \end{cases}$

VII. EXPERIMENTAL STUDY: APPLICATION TO PV SYSTEM

Several techniques in the literature have been applied specifically for PV integrated systems: Hybrid MPPT [23], open circuit voltage [24], short circuit current [25], predictive control approaches [26, 27], etc. These techniques rely on the PV model for optimization. The non-model based conventional ESC has also already been used to optimize the PV system. In [28], a comparative study was carried out between the methods used for the optimization of a PV system model. The study shows that the ESC scheme is more robust and efficient than other online optimization methods such as

Perturbation and observation method (P&O) with fixed perturbation size [29] or variable perturbation size [30].

The proposed approach ESC_a aims at developing a real time optimization technique that simultaneously insures good precision and speed of convergence towards the optimum operating point of a dynamic system subject to external disturbances. The approach is not intended specifically for a PV application, but can be applied to several other types of systems where the model is difficult to describe from physics laws. It has already been applied in simulations to a microbial fuel cell (MFC) model which is characterized by slower and much more complex dynamics than the one for PV systems. In [13], the ESC_a allowed the MFC system to converge towards the optimum with high accuracy and to gain days in terms of convergence time compared to the conventional ESC.

In the present study, the PV system was chosen to highlight the proposed approach and validate it experimentally because of its speed and practicality compared to MFC. The time of convergence towards the optimum of an MFC system is in terms of days while the time convergence of PV system is in term of seconds. Also, it is more accessible in the laboratory than an MFC. So, the comparative study between ESC and ESC_a will be established in the case of optimization of the power produced by a photovoltaic system. The optimal power produced by a PV is very sensitive to external disturbances, mainly sunlight radiations and temperature. According to [11], in real operating conditions, the influence of a temperature disturbance on the PV optimal power is negligible compared to the radiation disturbance. Hence, only the radiation is considered here as a measurable disturbance.

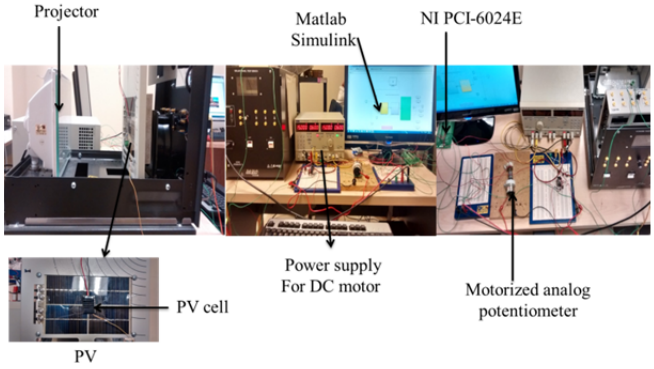

Fig. 3. Experimental platform.

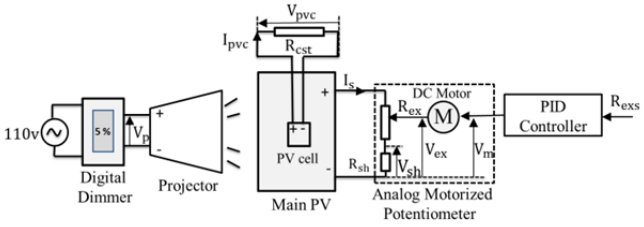

Fig. 4. Block diagram of the experimental platform.

A. Description of the experimental PV setup

As shown in Fig. 3 and Fig. 4, the experimental setup consists of:

- A PV module (Labvolt solar panel test bench, model 8805) permanently fixed in front of a 300 W projector acting as a light source;
- A digital touch screen dimmer (Uber Haus, TSD-1000) which allows to control the radiation emitted by the projector by adjusting its supply voltage (V_p) from 5% to 100% with a step of 5;
- A small photovoltaic cell (Solarbotics SCC2433B-MSE) which feeds a constant load (270 ohm) to evaluate the radiation disturbance based on the measurement of its output voltage;
- An analog motorized potentiometer constituted by a DC geared motor (Hsiang Neng DC Micro Motor Manufacturing Corporation, HN-GH35GMB) mechanically linked to an analog 1K potentiometer (Precision Electronics Corporation RV4NAYSD102A), playing the role of a variable external load (R_{ex}) at the output of the main PV module;
- An acquisition board (National Instrument NI PCI-6024E) which allows the measurement of the voltage at the PV module (V_{ex}), at the small photovoltaic cell (V_{pvc}) and at the shunt resistor $R_{sh} = 30$ ohm (V_{sh}) used to compute the power;
- A Matlab Simulink software for the implementation of the ESC and ESC_a schemes (sampling time: $T_s = 0.01$s).

A PID controller is used to adjust the DC geared motor supply voltage (V_m) in order to control the load value R_{ex} to the load setpoint (R_{exs}). The PID controller parameters have been adjusted following the analog motorized potentiometer model identification. This identification was performed using the Ident function in Matlab. The controller parameters have been chosen with the help of the auto-tune function provided with the PID Controller block from Simulink.

The PID controller form is parallel, the filter coefficient is 0.7611 and the proportional, integration and derivative gains were set respectively to $0.023\ V/\Omega$, $0.00213\ V/(\Omega s)$ and $0.0152\ Vs/\Omega$.

Considering the PV system described above, the optimization problem defined in (3) becomes:

$$\begin{aligned} &Max_{R_{exs}}\ P_s(R_{exs}) \\ &s.t.\quad \dot{x} = f(x, R_{exs}, G) = 0 \end{aligned} \tag{47}$$

where the radiation G is the measurable disturbance d_m, the PV power output in static mode, P_s, represents the objective function J, the state vector x includes the armature current, the supply voltage, the position and the speed of the DC motor and, β is the setpoint of the PID loop (R_{exs}).

In order to observe the effect of radiation on the PV optimal power (P_s^*), a variation in R_{ex} from 100 to 1000 ohm was performed with a step of 50 ohm for each level of radiation going from 100% to 10% with a step of 10%.

From Fig. 5 it can be seen that for each level of radiation, the optimal power P_s^* changes, and, not surprisingly, the PV generates its maximum power when the external load R_{ex} is equal to its internal load (R_{in}) (Table III). Thus, the motorized potentiometer will be controlled in order to match the internal load of the PV at each level of radiation.

As the external load is normally imposed to the PV system, a DC-DC converter is usually used to perform imped-

ance matching. Indeed, the duty cycle variation of a DCDC converter has a direct effect on the impedance seen by the PV source in the case where a fixed load is connected to the output of the DCDC converter. However, since the focus of our paper is more on the design of a new optimization method (applicable to other types of systems needing to be optimized in real-time), the experimental setup has been kept simple.

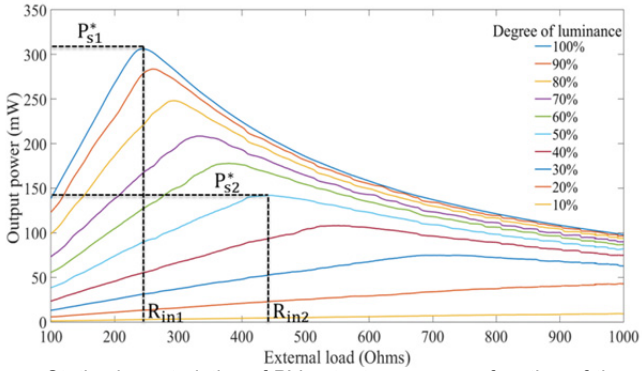

Fig. 5. Static characteristics of PV output power as a function of the external load for different radiation or luminance levels %.

The efficiency of both approaches (ESC and ESC_a) will be evaluated using the following efficiency factors used in many papers related to the optimization of renewable energy sources [31-33]: time of convergence (T_c), tracking efficiency (T_{eff}) and tracking accuracy in steady-state (T_{acc}). Note that the time of convergence will be evaluated both in terms of seconds and in terms of number of dither periods (N_p) in order to relate the performance to the optimization method rather than to the system itself. Hence, if a DCDC converter is used, the performance remains the same in terms of number of periods whereas the time of convergence (in seconds) is shorter than the one obtained with an analog potentiometer due to the faster dynamics of the system itself.

B. Performance of ESC and ESC_a under the radiation disturbance effect

In order to evaluate the ESC and ESC_a performance under the effect of the radiation, a variation of radiation will be performed at specific times by operating the digital dimmer from 100% to 50%. As shown in Fig. 5, these two levels of radiation correspond to two different optimal operating points: $R_{in1} = 244.4\ ohm, P_{s1}^* = 306{,}3\ mW$ for 100% of radiation and $R_{in2} = 447.9\ ohm\ , P_{s2}^* = 141.9\ mW$ for 50% of radiation. In such a situation, the role of the two optimization methods is to converge to the internal load of the PV system for each level of radiation by controlling the R_{ex} with the PID controller.

As shown in Section IV, the first step to implement the ESC_a technique is to model the effect of the external disturbance on the optimal operating point of the system. According to Table III the relation between the radiations generated by the projector and the PV internal resistance is a nonlinear relation. Therefore, as mentioned in Section IV, the proposed approach is to use a neural network model.

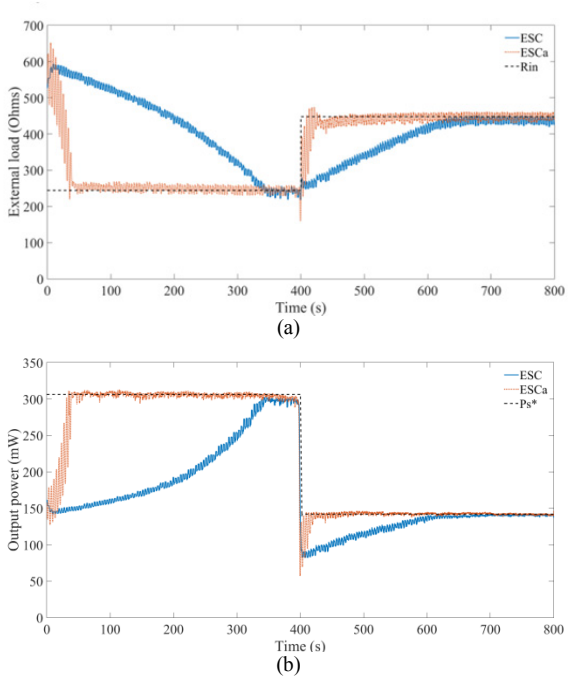

Fig. 6. Evolution of the system under ESC_a and ESC in situation 1 for a disturbance of radiation level going from 100% to 50% at T= 400 s: (a) external load and (b) external power.

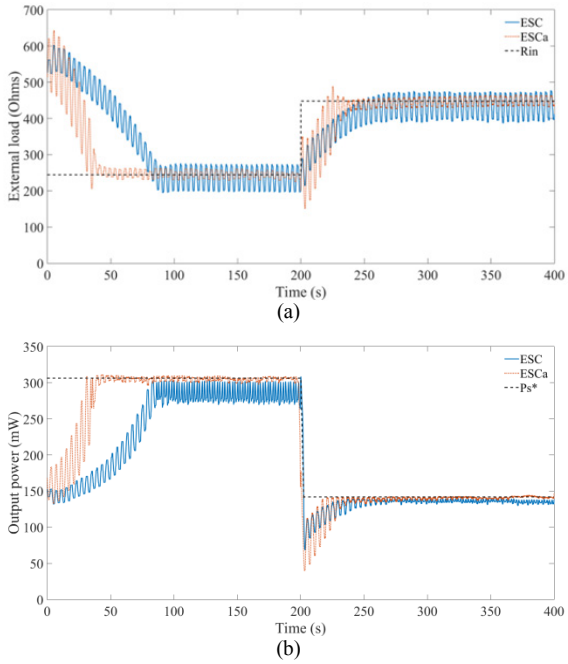

Fig. 7. Evolution of the system under ESC_a and ESC in situation 2 for a disturbance of radiation level going from 100% to 50% at T= 200 s: (a) external load and (b) external power.

The performance of NN model in terms of estimation accuracy depends directly on the richness of information contained in the dataset used during the training phase [34]. For systems such as PV, the rich data collection describing the relation between the optimal operating points and external disturbance (temperature, irradiation, etc.) can be performed by plotting the static power curves as a function of the control input (duty cycle, external load, etc.). This method indirectly gives a general idea of the effect of external perturba-

tion on the PV internal load. In such a condition, after the learning phase, the NN model offers very good accuracy in estimating the optimal control input of the system [28, 35].

TABLE III
OPTIMAL VALUES OF PV INTERNAL RESISTANCE AND OUTPUT POWER OF THE SMALL PV CELL AND NN MODEL OUTPUTS FOR DIFFERENT LUMINANCE LEVELS, I.E. DIFFERENT DIMMER POSITIONS

Relative position of the dimmer	Internal resistance R_{in} of PV (Ω)	Power of the PV cell P_{pvc}(mW)	Internal resistance estimated by NN (Ω)
100%	244	30.8	--
90%	230	26	235
80%	260	18.9	274
70%	300	13.2	--
60%	335	9.9	340
50%	447	6	--
40%	550	3.8	522
30%	695	1.7	--
20%	910	0.4	927
10%	990	0.18	--

In this study, the learning database is defined by the measurements shown in Table III which correspond to the following degrees of radiation: 100%, 70%, 50%, 30% and 10%. Once the learning phase is completed, the neural network model that describes the relation between R_{in} and P_{pvc} is represented by equations (13) to (17) where $d_m = P_{pvc}$, $\widehat{\beta^*} = \widehat{R_{in}}$, $h = 1$, $c = 10$ and $bias = 0.5$. The power of generalization test was performed to verify the model ability to estimate the PV internal resistance at degrees of radiations which differ from those used during the learning phase (results shown in Table III, column 4).

Note that the internal resistances estimated by NN for 100%, 70%, 50%, 30% and 10% degrees of irradiation have not been included in the fourth column of Table III since as these points were used during the learning phase of the NN model, the corresponding estimation error is negligible.

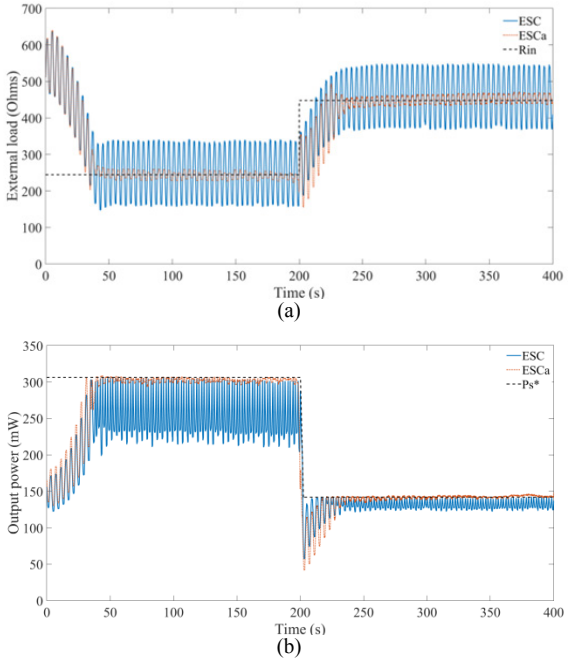

Fig. 8. Evolution of the system under ESC_a and ESC in situation 3 for a disturbance of radiation level from 100% to 50% at T= 200 s : (a) evolution of the external load and (b) external power.

Before the implementation of ESC or ESC_a, the control parameters are adjusted to respect the time scale separation condition between the system, the excitation signal and the filters. The entire system includes the motorized potentiometer, the PID controller and the PV panel itself. Compared to other components of the whole system, the PID controller is the slowest element, with an average response time of $T_{PID} = 1\ s$. Hence, the parameters of the two methods are selected according to the response time of the PID regulator.

The NN modeling is performed in two stages. The first step consists in training the NN model using the level of radiation (evaluated by measuring the output power of the small photovoltaic cell P_{pvc}) as an input and the corresponding internal resistance as the desired output (Table III). The second step is the test of NN generalization power.

Consequently, the ESC and ESC_a are designed as follows: the perturbation signal is a sinusoidal wave with frequency $F = 1/(4T_{PID}) = 0.25\ Hz$; the cutoff frequencies of the high pass and low pass filters are set to $\omega_l = \omega_h = 2F\pi/5 =$ 0.314 Hz and, the initial external load (at the integrator) is fixed to $R_{ini} = 500$ ohm.

In order to ensure the stability of the ESC and ESC_a loops, the combinations $a \times k_{ESC}$ and $\delta \times k_{ESC\,a}$ should be chosen such as to respect the conditions (39) with $\beta^* = R^*_{ex}$. In the present case, the stability conditions (39) are met by choosing $a \times k_{ESC}$ and $\delta \times k_{ESC\,a}$ to be less or equal to $\alpha_{max} = 0.5$. Note that this value of α_{max} was found by trial and error in order to ensure the stability of the closed-loop system.

As in the theoretical study, ESC scheme will be tested in the three situations described in Table I with $a_{min} = 25$ohm, $a_{max} = 100$ohm and $\mu = 2.5$. In the case of ESC_a the amplitude of the excitation signal δ will be switched from the same values a_{max} to a_{min} according to (9) with $e_{max} = 50$ ohm $\gg \mathrm{Max}\left(R_{in}(z) - \widehat{R}_{in}(z)\right)$, $z\{1,2,\ldots,N_g\}$, and N_g being the total number of points used for the generalization test (shown in Table III).

Since the system to be controlled remains the same, the values of high-pass and low-pass filters parameters and of the frequency of the excitation signal are identical for both ESC and ESC_a methods. Consequently, the gains k_{ESC} in ESC and k_{ESC_a} in ESC_a will be chosen based on the value of α_{max} in order to guarantee the maximum speed of convergence towards the optimum while respecting the stability condition (39). Thus, in order to guarantee the fastest possible convergence to the optimum for all values of a (Table I), $k_{ESC} = \alpha_{max}/a$ in each situation. In the case of ESC_a, since the amplitude of the excitation signal δ is variable, the gain $k_{ESC_a} = \alpha_{max}/a_{max}$ in all three situations in order to guarantee the maximum convergence speed towards the optimal operating point while respecting the stability condition (39) even when δ varies from a_{max} to a_{min}.

Fig. 6, 7, 8 and Table IV give a complete comparison between ESC_a and ESC performance in the three situations. In situation 1, ESC_a method converges nearly with the same tracking accuracy in steady state as the classical ESC one while it converges up to 8.4 times faster (when a 50% radiation disturbance occurs). In Situation 2, ESC_a approach converges more quickly and accurately than classic ESC loop.

Finally, in Situation 3, the ESC_a methods converges nearly within the same time toward the optimum (with a small delay however because e_{max} is slightly superior to $0.05\beta^* = 0.05R_{in}$) than the conventional ESC loop, but it provides a higher precision around the optimum.

Looking at equations (38) and (46), one can see that the choice of the amplitude, the initial point of operation and the curvature around the optimum will influence the time of convergence of both methods. Moreover, from these two equations, the theoretical time ratio $T_{ESC}/T_{ESCa} \approx a_{max}/a$ is equal to 4, 2 and 1 for situations 1, 2 and 3 respectively. In practice, from Table IV, the experimental convergence time ratios can be computed to be respectively equal to 7.3, 2 and 1 (when moving from R_{ini} to R_{in1}) and to 8.4, 1.7 and 1 (when moving from R_{in1} to R_{in2}). Hence, for situations 2 and 3, the experimental results are near the theoretical one whereas for situation 1, results differ. This can be explained by the fact that since the theoretical development provided in Section VI is based on a first order Taylor series expansion, it is valid around the optimum. However, in the experimental study, the system was started far away from its optimum. Since in situation 1, the convergence of the ESC method was slower, the system remains far from the optimum for a long period of time and it may be the reason why the experimental convergence time ratio differs from the theoretical one.

Note that in order to let the ESC method find enough time to converge to the desired optimum, the radiation disturbance was performed at 400 s in situation 1 (Fig. 6) rather than at 200s as in situations 2 (Fig. 7) and 3 (Fig. 8). Thus, since the parameters of ESC_a are identical in all three situations, the results shown for situations 2 and 3 were obtained from the same experiment whereas another experiment was required for situation 1. As a result, the values of the performance criteria for the ESC_a method slightly differs in situation 1 from the one obtained in situations 2 and 3.

When applied to a renewable energy source like PV, the precision and convergence time towards the optimum of the two optimization methods have a significant effect on the system performance in terms of energy production. Results depicted in Fig. 6 and Table IV show that in the first situation, the ESC scheme converges precisely towards the desired optimal operating point in steady state (good tracking accuracy) by bringing the external load around a value near to the internal resistance of the PV. However, the ESC technique takes a long time (large number of periods) to converge to the desired optimum if the initial external resistance is far from the PV internal resistance or if there is a significant variation of radiation. This slow convergence causes a decrease of the tracking efficiency which results in a loss of power. This can lead to a problem of inaccuracy if the disturbance frequency is high. In Situation 2, we can see from Fig. 7 and Table IV that if the designer makes a compromise between speed of convergence and accuracy by increasing the amplitude of the excitation signal from 25 to 50 ohm and adjusting the gain consequently (from 0.02 to 0.01), the convergence time decreases compared to Situation 1, but the precision around the optimum decreases as well. This choice of parameter values leads to an increase of the tracking efficiency but can cause a loss of power if the curvature of the static curve around the optimum is very stiff as it is the case when the radiation level is 100%. Finally, in Situation 3 (Fig. 8 and Table IV) if the expert favors speed over accuracy, the ESC loop converges very quickly to the desired optimum operating point, but the large oscillations around the internal resistance of the PV system generate a loss of power even when the curvature of the power static curve around the optimum is small as it is the case when the radiation level is 50%. Hence, the tracking efficiency is inferior to the one observed in Situation 2.

Most of the time, the expert designing an ESC scheme chooses Situation 2 in order to make a compromise between the time of convergence and the precision and obtain the best tracking efficiency. However, according to these results, it is not possible to ensure the best time of convergence and the best precision simultaneously. Hence the ESC_a parameter (excitation amplitude) is controlled in an adaptive manner in order to guarantee fast convergence and precision at the same time. Then, from Fig. 6, 7, 8 and Table IV with ESC_a the maximum tracking efficiency is guaranteed, therefore the PV system produces more power compared to ESC in three situations if the PV system is subject to radiation disturbance.

TABLE IV
PERFORMANCE EVALUATION OF ESC AND ESC_A APPROACHES

Optimization method		T_c from R_{ini} to R_{in1}(s)	T_c from R_{in1} to R_{in2} (s)	N_p from R_{ini} to R_{in1}	N_p from R_{in1} to R_{in2}	T_{acc} under P^*_{s1}(%)	T_{acc} under P^*_{s2}(%)	T_{eff} (%)
ESC	Situation 1	336.7	214.4	84.17	53.6	97.15	98.93	77.96
	Situation 2	85.76	54.4	21.44	13.6	93.05	96.63	86.15
	Situation 3	43.38	24.5	10.84	6.12	82.59	92.50	84.67
ESC_a	Situation 1	46.18	25.6	11.54	6.4	99.03	99.74	97.51
	Situation 2	43.7	31.3	10.92	7.82	99.44	99.41	93.72
	Situation 3	43.7	31.3	10.92	7.82	99.44	99.41	93.72

VIII. CONCLUSION

In this study, a modification of the classic ESC scheme was proposed in order to adapt the excitation signal amplitude using the power of neural network estimation. Theoretical and experimental results show that this approach is stable and significantly reduces the undesirable effects of the time-scale separation condition on the performance of the closed loop system while increasing the tracking efficiency. This method can contribute to achieve higher power performance for PVs or other renewable energy sources like microbial fuel cells, wind generators or any system which must be optimized subject to measurable external disturbances.

The neural network learning in this study is offline. Thus, if a non-measurable disturbance occurs, the accuracy of NN estimation may decrease. The objective of our next research

is to replace the offline NN-learning phase by an online NN adaptation in ESC_a, in order to increase the precision of NN estimation by providing a better adaptation of the NN model parameters under unmeasurable disturbances.

REFERENCES

[1] K. B. Ariyur and M. Krstic, *Real-time optimization by extremum-seeking control*: John Wiley & Sons, 2003.

[2] Y. Tan, W. Moase, C. Manzie, D. Nešić, and I. Mareels, "Extremum seeking from 1922 to 2010," in *Control Conference (CCC), 2010 29th Chinese*, 2010, pp. 14-26.

[3] C. Zhang and R. Ordóñez, *Extremum-seeking control and applications: a numerical optimization-based approach*: Springer Science & Business Media, 2011.

[4] A. Kebir, L. Woodward, and O. Akhrif, "Extremum-seeking control with anticipative action of microbial fuel cell's power," in *Control and Automation (MED), 2015 23th Mediterranean Conference on*, 2015, pp. 933-939.

[5] M. Guay and T. Zhang, "Adaptive extremum seeking control of nonlinear dynamic systems with parametric uncertainties," *Automatica,* vol. 39, pp. 1283-1293, 2003.

[6] R. Banavar, "Extremum seeking loops with quadratic functions: estimation and control," *International Journal of Control,* vol. 76, pp. 1475-1482, 2003.

[7] C. Zhang and R. Ordónez, "Numerical optimization-based extremum seeking control of LTI systems," in *Proceedings of the 44th IEEE Conference on Decision and Control*, 2005, pp. 4428-4433.

[8] V. Adetola, D. Dehaan, and M. Guay, "Adaptive extremum-seeking receding horizon control of nonlinear systems," in *American Control Conference, 2004. Proceedings of the 2004*, 2004, pp. 2937-2942.

[9] V. Adetola and M. Guay, "Adaptive output feedback extremum seeking receding horizon control of linear systems," *Journal of Process Control,* vol. 16, pp. 521-533, 2006.

[10] Y. Tan, D. Nešić, and I. Mareels, "On the choice of dither in extremum seeking systems: A case study," *Automatica,* vol. 44, pp. 1446-1450, 2008.

[11] S. Marinkov, B. de Jager, and M. Steinbuch, "Extremum seeking control with data-based disturbance feedforward," in *American Control Conference (ACC), 2014*, 2014, pp. 3627-3632.

[12] Y. Tan, D. Nešić, I. M. Mareels, and A. Astolfi, "On global extremum seeking in the presence of local extrema," *Automatica,* vol. 45, pp. 245-251, 2009.

[13] A. Kebir, O. Akhrif, and L. Woodward, "Extremum-seeking control of a microbial fuel cell power using adaptive excitation," in *Industrial Electronics Society, IECON 2016-42nd Annual Conference of the IEEE*, 2016, pp. 4127-4132.

[14] K. Liu and Z.-Q. Zhu, "Position-offset-based parameter estimation using the adaline NN for condition monitoring of permanent-magnet synchronous machines," *IEEE Transactions on Industrial Electronics,* vol. 62, pp. 2372-2383, 2015.

[15] L. Haijun, W. Lucai, T. Zhaosheng, D. Houde, and L. Songhui, "Optimization for a Neural Network Based on Input-Vectors Correlation and Its Application to a Truck Scale," *IEEE TRANSACTIONS ON INDUSTRIAL ELECTRONICS,* 2017.

[16] N. J. Cotton and B. M. Wilamowski, "Compensation of nonlinearities using neural networks implemented on inexpensive microcontrollers," *IEEE Transactions on Industrial Electronics,* vol. 58, pp. 733-740, 2011.

[17] R. Zhang and J. Tao, "Data driven modeling using improved multi-objective optimization based neural network for coke furnace system," *IEEE Transactions on Industrial Electronics,* 2016.

[18] C. M. Bishop, *Neural networks for pattern recognition*: Oxford university press, 1995.

[19] H. K. Khalil, *Nonlinear systems*, 2nd ed. ed. Upper Saddle River, N.J.: Prentice-Hall, 1996.

[20] R. A. DeCarlo, M. S. Branicky, S. Pettersson, and B. Lennartson, "Perspectives and results on the stability and stabilizability of hybrid systems," *Proceedings of the IEEE,* vol. 88, pp. 1069-1082, 2000.

[21] R. Shorten and K. Narendra, "On the stability and existence of common Lyapunov functions for stable linear switching systems," in *Decision and Control, 1998. Proceedings of the 37th IEEE Conference on*, 1998, pp. 3723-3724.

[22] H. K. Khalil, *Nonlinear systems*, 3rd ed. ed. Upper Saddle River, N.J.: Prentice Hall, 2002.

[23] M. H. Moradi and A. R. Reisi, "A hybrid maximum power point tracking method for photovoltaic systems," *Solar Energy,* vol. 85, pp. 2965-2976, 2011.

[24] J. H. Enslin, M. S. Wolf, D. B. Snyman, and W. Swiegers, "Integrated photovoltaic maximum power point tracking converter," *IEEE Transactions on Industrial Electronics,* vol. 44, pp. 769-773, 1997.

[25] T. Noguchi, S. Togashi, and R. Nakamoto, "Short-current pulse-based maximum-power-point tracking method for multiple photovoltaic-and-converter module system," *IEEE Transactions on Industrial Electronics,* vol. 49, pp. 217-223, 2002.

[26] W. Qi, J. Liu, X. Chen, and P. D. Christofides, "Supervisory predictive control of standalone wind/solar energy generation systems," *IEEE transactions on control systems technology,* vol. 19, pp. 199-207, 2011.

[27] K. Rahbar, J. Xu, and R. Zhang, "Real-time energy storage management for renewable integration in microgrid: An off-line optimization approach," *IEEE Transactions on Smart Grid,* vol. 6, pp. 124-134, 2015.

[28] A. R. Reisi, M. H. Moradi, and S. Jamasb, "Classification and comparison of maximum power point tracking techniques for photovoltaic system: A review," *Renewable and Sustainable Energy Reviews,* vol. 19, pp. 433-443, 2013.

[29] V. Salas, E. Olias, A. Lazaro, and A. Barrado, "Evaluation of a new maximum power point tracker (MPPT) applied to the photovoltaic stand-alone systems," *Solar energy materials and solar cells,* vol. 87, pp. 807-815, 2005.

[30] G. Yu, Y. Jung, J. Choi, and G. Kim, "A novel two-mode MPPT control algorithm based on comparative study of existing algorithms," *Solar Energy,* vol. 76, pp. 455-463, 2004.

[31] N. Bizon, "Global Extremum Seeking Control of the power generated by a Photovoltaic Array under Partially Shaded Conditions," *Energy Conversion and Management,* vol. 109, pp. 71-85, 2016.

[32] Y. Wang, Y. Li, and X. Ruan, "High-accuracy and fast-speed MPPT methods for PV string under partially shaded conditions," *IEEE Transactions on Industrial Electronics,* vol. 63, pp. 235-245, 2016.

[33] O. Khan and W. Xiao, "Integration of Start–Stop Mechanism to Improve Maximum Power Point Tracking Performance in Steady State," *IEEE Transactions on Industrial Electronics,* vol. 63, pp. 6126-6135, 2016.

[34] T. Esram and P. L. Chapman, "Comparison of photovoltaic array maximum power point tracking techniques," *IEEE Transactions on energy conversion,* vol. 22, pp. 439-449, 2007.

[35] M. C. Di Piazza and M. Pucci, "Induction-Machines-Based Wind Generators With Neural Maximum Power Point Tracking and Minimum Losses Techniques," *IEEE Transactions on Industrial Electronics,* vol. 63, pp. 944-955, 2016.

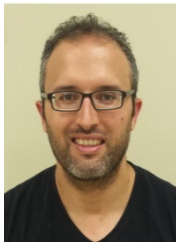

Anouer Kebir (S'12) received the B. Sc. degree in electrical engineering and the M. Sc. degree in automatic control and production engineering from the École nationale supérieure d'ingénieurs de Tunis, Tunisia in 2008 and 2012 respectively. In 2013, he also received the B. Sc. degree in telecommunications engineering from the École nationale d'ingénieurs de Tunis, Tunisia. He is currently working toward the PhD degree in electrical engineering at the École de technologie supérieure in Montreal, Canada. He is a member of GREPCI (Groupe de Recherche en Commande Industrielle et Électronique de Puissance). His research interests include artificial intelli-

gence, image processing, biomechanics, real-time optimization and control of solar energy and bioenergy.

Lyne Woodward (M'12) received the B. Sc. degree in Electrical Engineering from the University of Sherbrooke, Quebec, Canada in 1994. From 1995 to 2004, she worked as engineer in the process control department of Hatch. She obtained the M. Sc. A. and Ph. D. degrees in Chemical Engineering from "Ecole Polytechnique de Montréal", Quebec, Canada in 2003 and 2009 respectively. Since 2010, she has been an Associate Professor in the Electrical Engineering department of the "École de technologie supérieure", Montreal, Canada. She is also the director of the GREPCI (« Groupe de Recherche en Commande Industrielle et Électronique de Puissance »), a research group working on power electronics and industrial control which includes more than a hundred of members. Her research interests include real-time optimization, control of linear and nonlinear systems, optimal conversion and management of renewable energy such as wind energy, solar energy, bioenergy.

Ouassima Akhrif (M'93) received the M.Sc (87') and Ph.D (89') in Electrical Engineering, Control Systems at University of Maryland, College Park, USA.
She was Assistant professor at Systems Engineering Department, Case Western Reserve University in Cleveland. In 1992, she joined the "École de Technologie Supérieure", University of Québec in Montréal, Canada, where she is currently a Full Professor in the Electrical Engineering Department. She is a member of GREPCI (Groupe de Recherche en Commande Industrielle et Électronique de Puissance), a research group that she directed from 2004 to 2009. Her research interests are bifurcation analysis, nonlinear geometric control, nonlinear adaptive control and their applications in electric drives, power systems, renewable energy integration, autopilot design and flight control systems.